Available online at www.sciencedirect.com
SCIENCE DIRECT®
PERGAMON
Polyhedron 22 (2003) 2885–2894
POLYHEDRON
www.elsevier.com/locate/poly

Crystal structures and solution dynamics of monocyclopentadienyl titanium(IV) complexes bearing pendant ether and phosphanyl type functionalities

Dmitrii P. Krut'ko [a,*], Maxim V. Borzov [a], Eduard N. Veksler [a], Andrei V. Churakov [b], Karel Mach [c]

[a] *Department of Chemistry, M.V. Lomonosov Moscow State University, Leninskie Gory, Moscow 119899, Russia*
[b] *N.S. Kurnakov Institute of General and Inorganic Chemistry, Russian Academy of Science, Russia*
[c] *J. Heyrovský Institute of Physical Chemistry, Academy of Sciences of the Czech Republic, Czech Republic*

Received 13 March 2003; accepted 23 May 2003

Abstract

Two novel half-sandwich Ti(IV) complexes, $[\eta^5{:}\eta^1\text{-}O\text{-}C_5(CH_3)_4CH_2CH_2OCH_3]TiCl_3$ (**3**) and $(\eta^5{:}\eta^1\text{-}P\text{-}C_5H_4CH_2CH_2PPh_2)TiCl_3$ (**6**), were prepared and structurally characterised. At elevated temperatures, complex **3** undergoes a conversion into $[\eta^5{:}\sigma\text{-}C_5(CH_3)_4CH_2CH_2O\text{–}]TiCl_2$ (**4**). The dynamic behaviour of complexes **3** and **6** in solutions has been studied by variable-temperature ^1H, ^{13}C and ^{31}P NMR spectroscopy. Thermodynamic parameters of the intramolecular dissociation-coordination processes for **3** and **6** were elucidated by the numerical analysis of the $\delta(T)$ dependencies. The intramolecular M(IV)←E (M = Ti, Zr; E = O, P) coordination in half-sandwich cyclopentadienyl complexes is discussed.

Keywords: Titanium; Cyclopentadienyl ligands; Intramolecular coordination; O ligands; P ligands; Variable-temperature NMR spectroscopy

1. Introduction

The cyclopentadienyl complexes of transition metals possessing chelating heterofunctional side-chain groups form an important class of organometallic compounds and are now under intense investigation (see recent reviews [1–3]). Among these compounds, monocyclopentadienyl-type complexes of the Group 4 metals attract a particular interest, mostly due to their known ability to be applied as precursors of catalysts for α-olefin polymerisation.

Besides this practical interest, the Group 4 metal half-sandwiches exhibit a rich coordination chemistry. In many cases, peculiarities of the spatial organisation of these complexes and details of their dynamic behaviour in solutions are unpredictable and are of common theoretical value.

During recent years our research team performed systematic studies of Zr(IV) complexes derived from $C_5H_4CH_2CH_2PPh_2$ [4], $C_5(CH_3)_4CH_2CH_2OCH_3$ [5], $C_5(CH_3)_4CH_2CH_2SCH_3$ [6], $C_5(CH_3)_4CH_2CH_2N(CH_3)_2$ [7], $C_5(CH_3)_4CH_2CH_2P(CH_3)_2$ [7] and $C_5(CH_3)_4$-$CH_2CH_2PPh_2$ [7,8] ligands. Here we report our results on the synthesis, structural and dynamic behaviour investigation of two novel mono-cyclopentadienyl complexes of titanium(IV): $(\eta^5{:}\eta^1\text{-}C_5H_4CH_2CH_2PPh_2)TiCl_3$ and $(\eta^5{:}\eta^1\text{-}C_5(CH_3)_4CH_2CH_2OCH_3)TiCl_3$.

2. Experimental

2.1. General remarks

All procedures were performed in sealed-off evacuated glass vessels. The employed solvents (and their perdeuterated analogues) were dried with and distilled from conventional agents (namely: diethyl ether and THF—with sodium benzophenone ketyl; toluene, hep-

* Corresponding author. Tel.: +7-095-939-1234; fax: +7-095-932-8846.
E-mail address: kdp@org.chem.msu.su (D.P. Krut'ko).

0277-5387/03/$ - see front matter © 2003 Elsevier Ltd. All rights reserved.
doi:10.1016/S0277-5387(03)00407-8

tane and pentane—with Na–K alloy; CH_2Cl_2—with P_2O_5 and then with CaH_2). When performing procedures in evacuated vessels, the degassed solvents were stored in evacuated reservoirs over the corresponding drying agent and transferred on a high vacuum line directly into reaction vessels by trapping with liq. N_2. Trimethylchlorosilane (Fluka) was refluxed with and distilled from aluminium powder (high vacuum line); titanium tetrachloride was refluxed over freshly reduced copper powder, degassed and distilled on a high vacuum line (Teflon grease must be applied). $HC_5(CH_3)_4$–$CH_2CH_2OCH_3$ and $(CH_3)_3Si$–C_5H_4–$CH_2CH_2PPh_2$ were prepared accordingly to the reported procedures. ^1H, ^{13}C and ^{31}P NMR spectra were recorded on a Varian VXR-400 spectrometer at 400, 100 and 162 MHz, respectively. For ^1H and $^{13}C\{^1H\}$ spectra, solvent resonances [$\delta_H = 7.15$ and $\delta_C = 128.0$ (C_6D_6), $\delta_H = 5.32$ and $\delta_C = 53.8$ (CD_2Cl_2), $\delta_H = 1.73$ and $\delta_C = 25.3$ (THF-d_8)] were used as internal reference standards. For $^{31}P\{^1H\}$ spectra, 85% H_3PO_4 was employed as an external reference. For temperature calibration, the standard methanol and ethyleneglycol samples were used. The elemental analyses were performed on the Carlo-Erba automated analyser. Mass spectra were measured on Kratos-MS-890 and Varian MAT CH7a Fa spectrometers.

2.2. Synthetic procedures

2.2.1. $(CH_3)_3Si$–$C_5H_4CH_2CH_2OCH_3$ (2)

A 1.6 M solution of *n*-BuLi in hexane (17.85 ml, 28.56 mmol) was added to a solution of cyclopentadiene $HC_5(CH_3)_4CH_2CH_2OCH_3$ (5.15 g, 28.57 mmol) in THF (60 ml) at 0 °C under stirring. The mixture was allowed to warm up to room temperature (r.t.) and left overnight. The resultant red–brown liquor was heated on a water bath and concentrated by trapping of the solvents into a vessel cooled with liq. N_2 until the precipitation of the solid from the hot solution started. The mixture was allowed to crystallise for 1 day, the white crystalline solid was filtered off, washed on a filter two times with 60 ml portions of cold ether, dried on a high-vacuum line and dissolved in 60 ml of THF (nearly colourless solution). To this solution heated on a boiling water bath, $(CH_3)_3SiCl$ (3.60 g, 28.57 mmol) was added at once and the reaction mixture was heated at 90–100 °C for 2 h. Formation of LiCl as well-formed snow-white crystals was observed (LiCl exhibits the inverted temperature dependence of solubility in THF; the observed crystalline precipitate dissolves on cooling the mixture back to the r.t.). The solvent and unreacted trimethylchlorosilane was removed under high vacuum and the residual yellow oil subjected to a bulb-to-bulb high vacuum distillation, that gave 2.34 g of trimethylsilyl substituted cyclopentadiene **2** as a pale-yellow oil. Yield 32.4%. A mixture of isomers. GC/MS EI (70 eV) *m/z* (%): 252 (18.5) [$M^{+\bullet}$], 237 (0.8) [$M^{+\bullet}-CH_3$], 207 (4.6) [$M^{+\bullet}-CH_2OCH_3$], 178 (4.0) [$M^{+\bullet}-HSi(CH_3)_3$], 148 (16.6) [$M^{+\bullet}-CH_3OSi(CH_3)_3$], 133 (100) [$C_7H_4(CH_3)_3^+$], 119 (15.4) [$C_7H_5(CH_3)_2^+$], 105 (7.0) [$C_7H_6(CH_3)^+$], 91 (8.4) [$C_7H_7^+$], 73 (49.9) [$Si(CH_3)_3^+$], 59 (7.7) [$CH_2CH_2OCH_3^+$], 45 (20.1) [$CH_2OCH_3^+$]. *Anal.* Found: C, 71.70; H 11.39. Calc. for $C_{15}H_{28}OSi$ (252.47): C, 71.36; H 11.18%. ^1H NMR (400 MHz, C_6D_6, 30 °C, δ ppm): −0.12 [br, $Si(CH_3)_3$], 1.16 [br, $CH_3C(Si(CH_3)_3$], 1.78, 1.82 (each br, $=CCH_3$), 2.28 [br, $OCH_2CH_2C(Si(CH_3)_3$], 2.65, 2.83 (each br, $=CCH_2CH_2O$), 3.15 (br s, OCH_3), 3.32 (br, OCH_2).

2.2.2. $(\eta^5:\eta^1$-O-$C_5H_4CH_2CH_2OCH_3)TiCl_3$ (3)

Silane **2** (2.34 g, 9.27 mmol) was dissolved in toluene (50 ml), mixed rapidly with a solution of $TiCl_4$ (1.76 g, 9.28 mmol) in toluene (10 ml) at −78 °C, then the mixture was allowed to warm up to r.t. and left overnight. The mixture was then heated at 70 °C for 1 h, the solvent removed under high vacuum and the residual solid recrystallised from ether. Yield of crude **3** (contaminated with unreacted $TiCl_4$) 1.70 g (55.0%). A part of the crude **3** was subjected to high-vacuum sublimation (10^{-3} torr, 150–170 °C). EI MS (70 eV) *m/z* (%): 332 (1.5) [$M^{+\bullet}$], 297 (22) [$M^{+\bullet}-Cl$], 296 (8) [$M^{+\bullet}-HCl$], 252 (19) [$M^{+\bullet}-Cl-CH_2OCH_3$], 179 (6) [$C_5(CH_3)_4CH_2CH_2OCH_3^+$], 149 (6) [$C_7H_4(CH_3)_2(O-CH_3)^+$], 148 (40) [$C_5(CH_3)_4CH_2CH_2^{+\bullet}$], 147 (47) [$C_7H_3(CH_3)_4^+$], 135 (10) [$C_7H_5(CH_3)(OCH_3)^+$], 134 (54) [$C_5(CH_3)_4{=}CH_2^{+\bullet}$], 133 (100) [$C_7H_4(CH_3)_3^+$], 121 (33) [$C_7H_6(OCH_3)^+$], 119 (52) [$C_7H_5(CH_3)_2^+$], 105 (18) [$C_7H_6(CH_3)^+$], 91 (27) [$C_7H_7^+$], 77 (14) [$C_6H_5^+$], 45 (59) [$CH_2OCH_3^+$]. *Anal*. Found: C, 42.81; H, 5.83. Calc. for $C_{12}H_{19}Cl_3OTi$ (333.52): C, 43.22; H, 5.74%. ^1H NMR (400 MHz, THF-d_8, 30 °C, δ ppm): 2.37, 2.39 [each s, 6H, $C_5(CH_3)_4$], 3.11 (t, 2H, $^3J_{HH} = 6.1$ Hz, CH_2CH_2O), 3.24 (s, 3H, OCH_3), 3.51(t, 2H, $^3J_{HH} = 6.1$ Hz, CH_2O). ^{13}C NMR (100 MHz, THF-d_8, 30 °C, δ ppm): 14.44, 14.70 (each q, $^1J_{CH} = 129$ Hz, $C_5(CH_3)_4$), 30.37 (t, $^1J_{CH} = 130$ Hz, CH_2CH_2O), 59.05 (q, $^1J_{CH} = 141$ Hz, OCH_3), 73.16 (t, $^1J_{CH} = 143$ Hz, CH_2O), 138.92, 139.26 (each s, C^{2-5}), 140.31 (s, C^1). ^1H NMR (400 MHz, CD_2Cl_2, 30 °C, δ ppm): 2.39, 2.41 [each s, 6H, $C_5(CH_3)_4$], 3.10 (t, 2H, $^3J_{HH} = 6.4$ Hz, CH_2CH_2O), 3.32 (s, 3H, OCH_3), 3.61 (t, 2H, $^3J_{HH} = 6.4$ Hz, CH_2O). $^{13}C\{^1H\}$ NMR (100 MHz, CD_2Cl_2, 30 °C, δ ppm): 14.75, 14.91 [$C_5(CH_3)_4$], 29.41 (CH_2CH_2O), 59.71 (OCH_3), 73.60 (CH_2O), 139.02, 139.04 (C^{2-5}), 140.67 (C^1). ^1H NMR (400 MHz, CD_2Cl_2, −69 °C, δ ppm): 2.31, 2.38 (each s, 6H, $C_5(CH_3)_4$), 2.93 (t, 2H, $^3J_{HH} = 6.4$ Hz, CH_2CH_2O), 3.50 (s, 3H, OCH_3), 4.27 (t, 2H, $^3J_{HH} = 6.4$ Hz, CH_2O). $^{13}C\{^1H\}$ NMR (100 MHz, CD_2Cl_2, −69 °C, δ ppm): 14.76 [$C_5(CH_3)_4$], 24.83 (CH_2CH_2O), 63.12 (OCH_3), 80.60 (CH_2O), 136.90, 137.50 (C^{2-5}), 145.62 (C^1).

2.2.3. (η^5:η^1-P-$C_5H_4CH_2CH_2PPh_2$)$TiCl_3$ (6)

Solutions of (3.39 g, 9.67 mmol) silane **5** (3.39 g, 9.67 mmol) in toluene (10 ml) and $TiCl_4$ (1.47 g, 7.70 mmol) in 20 ml of the same solvent were mixed at r.t. A deep red (purple) coloration appeared immediately. In 15 min the first orange crystals appeared. The reaction mixture was left overnight, the bulky yellow–orange crystalline precipitate was filtered off, washed with 30 ml of toluene, recrystallised from 10 ml of THF (slow cooling of the solution from 100 to 0 °C), washed with 30 ml of ether, and dried under high vacuum. Yield 2.24 g, 55.2%. An adduct with one molecule of toluene (even if recrystallised from THF). EI MS (70 eV) *m/z* (%): 430 (not observed) [$M^{+\bullet}$], 395 (86) [$M^{+\bullet}-Cl$], 360 (6) [$M^{+\bullet}-2Cl$], 277 (100) [$C_5H_4CH_2CH_2PPh_2^+$], 200 (7) [$C_5H_4CH_2CH_2PPh^{+\bullet}$], 199 (13) [$CH_2PPh_2^+$], 185 (28) [$PPh_2^+$], 183 (60) [$C_{12}H_8P^+$, (9-phosphafluorene-H)], 121 (49) [$CH{=}PPh^+$], 108 (34) [$PPh^{+\bullet}$], 91 (47) [$C_7H_7^{+\bullet}$], 77 (21) [$C_6H_5^+$]. *Anal*. Found: C, 59.51; H, 5.17. Calc. for $C_{26}H_{26}Cl_3PTi$ (523.70): C, 59.63; H, 5.00%. ^{1}H NMR (400 MHz, CD_2Cl_2, 30 °C, δ ppm; toluene signals are omitted): 3.20–3.29 (m, 4H, CH_2CH_2P), 6.67 (d of virtual t, 2H, $^{3+4}J_{HH} = 5.2$ Hz, $^5J_{HP} = 1.2$ Hz, $H^{2,5}$), 6.83 (virtual t, 2H, $^{3+4}J_{HH} = 5.2$ Hz, $H^{3,4}$), 7.39–7.48 (m, 6H, *m*- and *p*-H in PPh_2), 7.66 (m, 4H, *o*-H in PPh_2). ^{13}CNMR (100 MHz, CD_2Cl_2, 30 °C, δ ppm): 24.98 (dt, $^1J_{CH} = 133$ Hz, $^2J_{CP} = 10.7$ Hz, CH_2CH_2P), 34.07 (dt, $^1J_{CH} = 135$ Hz, $^1J_{CP} = 23.6$ Hz, CH_2P), 123.47, 123.50 (each d, $^1J_{CH} = 180$ Hz, C^{2-5}), 129.51 (dd, $^1J_{CH} = 161$ Hz, $^3J_{CP} = 8.6$ Hz, *m*-C in PPh_2), 130.92 (d, $^1J_{CH} = 161$ Hz, *p*-C in PPh_2), 133.13 (dd, $^1J_{CH} = 160$ Hz, $^2J_{CP} = 8.1$ Hz, *o*-C in PPh_2), 133.95 (d, $^1J_{CP} = 28.0$ Hz, *ipso*-C in PPh_2), 144.16 (d, $^3J_{CP} = 8.4$ Hz, C^1). ^{31}P-{^{1}H} NMR (162 MHz, CD_2Cl_2, 30 °C, δ ppm): 27.1 (s).

2.3. X-ray crystallographic study

Crystal data and data-collection information as well as a description of the structural analysis and refinement for compounds **3** and **6** are given in Table 1.

3. Discussion

3.1. O-Functionalized compounds

3.1.1. Synthesis

The titanium(IV) half-sandwich complex (η^5:η^1-$C_5(CH_3)_4CH_2CH_2OCH_3$)$TiCl_3$ (**3**) was prepared in two steps starting from lithium cyclopentadienide (**1**) via trimethylsilylated cyclopentadiene (**2**) in a good overall yield (see Scheme 1).

Initially cyclopentadiene [9] and its lithiated derivative **1** [5] were prepared as reported previously. Salt **1** smoothly reacts with $(CH_3)_3SiCl$ in THF at an elevated temperature (80–90 °C) giving the intermediate silane **2**. It is noteworthy that all attempts to perform the same silylation reaction in diethyl ether failed. Silane **2** was additionally purified by a high-vacuum distillation. A moderate yield of silane **2** [32% with respect to cyclopentadiene $HC_5(CH_3)_4CH_2CH_2OCH_3$] is due to the fact that the cyclopentadiene itself, if prepared according to literature procedure [9], is actually a crude product. Attempts to purify it by high-vacuum distillations gave poor results. Thus, isolation and purification of the lithium derivative **1** appeared to be inevitable.

Treatment of silane **2** with $TiCl_4$ in toluene under mild conditions (−78 to 20 °C) produced the desired half-sandwich complex **3**. Compound **3** was obtained as a bright-red crystalline solid, readily soluble in polar halocarbon solvents, THF and toluene. However, the product **3** is contaminated by residual non-reacted $TiCl_4$. Thus, in CD_2Cl_2 or $CDCl_3$ solutions, two sets of proton signals, that correspond to [η^5:η^1-*O*-$C_5(CH_3)_4CH_2CH_2OCH_3$]$TiCl_3$ (**3**) and its adduct with $TiCl_4$ were observed. In THF-d_8, however, the same crude **3** exhibits only one set of signals, that is indicative of the decomposition of the **3**·$TiCl_4$ adduct in a solvating medium.

The final purification of **3** from $TiCl_4$ can be achieved by a high-vacuum sublimation. However, if overheated under lower vacuum conditions, complex **3** converts into an ancillary cyclopentadienyl-alkoxide complex [η^5:σ-*O*-$C_5(CH_3)_4CH_2CH_2O$-]$TiCl_2$ (**4**), with an equivalent of CH_3Cl evolved (see Scheme 2).[1]

A similar process of the thermal interconversion was observed formerly by J.H. Teuben et al. [10] for a close analogue of **3**, [η^5:η^1-*O*-$C_5(CH_3)_4CH_2CH_2CH_2OCH_3$]$TiCl_3$, at 225 °C in toluene solution.

3.1.2. X-ray structural investigation of 3

A single crystal of **3** suitable for X-ray analysis was obtained by a high-vacuum sublimation. Contrarily to what observed for its Zr(IV) analogue, which was proved to form a dimeric (μ-Cl)$_2$ bridged structures with the metal centre possessing a distorted octahedral coordination [5], in complex **3** the Ti(IV) centre coordination polyhedron is a tetragonal pyramid assuming Cp to occupy one coordination site (see Fig. 1).

[1] Analyses data for (η^5:σ-$C_5(CH_3)_4CH_2CH_2O$–)$TiCl_2$ (**4**): ^{1}H NMR (400 MHz, C_6D_6, 30 °C): $\delta = 1.89$, 1.99 (both s, 12H, $(CH_3)_4C_5$); 2.55 (t, 2H, $^3J_{HH} = 7.1$ Hz, CH_2CH_2OTi), 5.17 (t,, 2H, $^3J_{HH} = 7.1$ Hz, CH_2CH_2OTi); ^{13}C–{^{1}H} NMR (100 MHz, C_6D_6, 30 °C): $\delta = 12.78$, 13.13 ($(CH_3)_4C_5$); 28.76 (CH_2CH_2OTi), 94.65 (OCH_2), 133.55 (H_3C-C_{ring}, the second signal is not observed), 141.32 ($-H_2C-C_{ring}$). MS EI (70 eV) *m/z* (%): 282 (14) [$M^{+\bullet}$], 254 (71) [$M^{+\bullet}-CH_2CH_2$], 252 (100) [$M^{+\bullet}-CH_2O$], 217 (7) [$M^{+\bullet}-CH_2O-Cl$], 216 (20) [$M^{+\bullet}-CH_2O-HCl$], 134 (11) [$(CH_3)_4C_5{=}CH_2^{+\bullet}$], 133 (13) [$C_7H_4(CH_3)_3^{+\bullet}$], 119 (22) [$C_7H_5(CH_3)_2^{+\bullet}$], 91 (10) [$C_7H_6(CH_3)^{+\bullet}$].

Table 1
Crystal data, data collection, structure solution and refinement parameters for complexes **3a** and **6**

Compound	$[\eta^5{:}\eta^1\text{-}O\text{-}C_5(CH_3)_4CH_2CH_2OCH_3]TiCl_3$ (**3a**)	$[\eta^5{:}\eta^1\text{-}P\text{-}C_5H_4CH_2CH_2PPh_2]TiCl_3 \cdot 1/2CH_2Cl_2$ (**6**)
Empirical formula	$C_{12}H_{19}Cl_3OTi$	$C_{19.5}H_{19}Cl_4PTi$
Formula weight	333.52	474.02
Color, habit	red needle	red block
Crystal size (mm)	$0.5 \times 0.2 \times 0.1$	$0.5 \times 0.4 \times 0.2$
Crystal system	orthorhombic	monoclinic
Space group	$Pna2_1$	$C2/c$
Unit cell dimensions		
a (Å)	14.562(5)	15.793(4)
b (Å)	8.267(4)	7.947(2)
c (Å)	12.338(13)	32.77(3)
β (°)		92.78(6)
V (Å^{-3})	1485(2)	4109(4)
Z	4	8
D_{calc} (g cm^{-3})	1.491	1.533
Absorption coefficient (mm^{-1})	1.098	1.016
$F(000)$	688	1928
Diffractometer	Enraf–Nonius CAD-4	Enraf–Nonius CAD-4
Temperature (K)	293	293
Radiation (λ (Å))	graphite monochromated Mo Kα (0.71073)	graphite monochromated Mo Kα (0.71073)
θ Range (°)	2.80 to 24.94	2.49 to 24.97
Index ranges	$-3 \le h \le 17,\ -9 \le k \le 2,\ -14 \le l \le 3$	$-18 \le h \le 18,\ -2 \le k \le 9,\ -4 \le l \le 38$
Reflections collected	2793	5520
Independent reflections	1753 ($R_{int} = 0.0247$)	3614 ($R_{int} = 0.0253$)
Absorption correction	none	empirical
Min. and max. transmission		0.5070 and 0.5731
Solution method	direct methods (SHELX-86) [16]	direct methods (SHELX-86) [16]
Refinement method	full-matrix least-squares on F^2 (SHELXL-93) [17]	full-matrix least-squares on F^2 (SHELXL-93) [17]
Hydrogen treatment	all H atoms were placed in calculated positions and refined using a riding model	all H atoms were placed in calculated positions and refined using a riding model
Data/restraints/parameters	1714/1/160	3423/0/307
Goodness-of-fit on F^2	1.075	1.054
Final R indices [$I > 2\sigma(I)$]	$R_1 = 0.0257$, $wR_2 = 0.0631$	$R_1 = 0.0389$, $wR_2 = 0.1025$
R indices (all data)	$R_1 = 0.0410$, $wR_2 = 0.0711$	$R_1 = 0.0788$, $wR_2 = 0.1231$
Absolute structure parameter	0.01(4)	–
Extinction coefficient	0.0057(11)	–
Largest difference peak and hole (e Å^{-3})	0.479 and −0.253	0.561 and −0.386

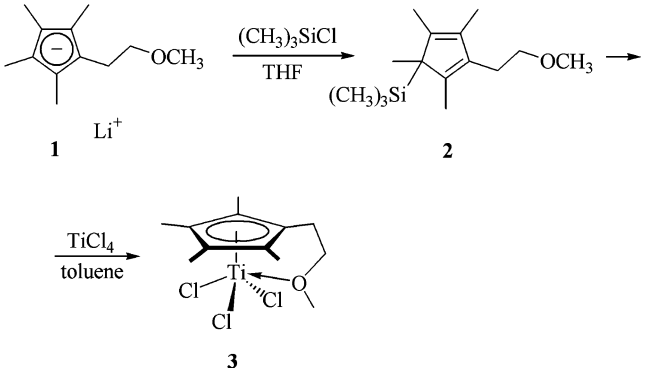

Scheme 1.

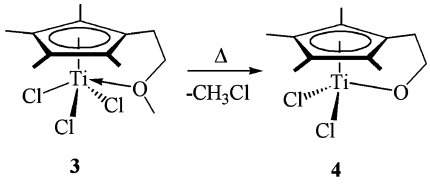

Scheme 2.

The oxygen moiety occupies one of the positions at the base of the pyramid. In general features, the molecular structure of **3** is close to that observed for its ring non-permethylated analogue $[\eta^5{:}\eta^1\text{-}O\text{-}C_5H_4CH_2CH_2OCH_3]TiCl_3$ [11]. However, comparatively to $[\eta^5{:}\eta^1\text{-}O\text{-}C_5H_4CH_2CH_2OCH_3]TiCl_3$ all the distances in the pseudo-five-membered metallocycle Ti–Cp_{cent}–C(6)–C(7)–O–(Ti) in **3** are somewhat longer [Ti–Cp_{cent} 2.046 vs. 2.028 Å, C(1)–C(6) 1.503(5) vs. 1.442(24) Å, C(6)–C(7) 1.510(6) vs. 1.477(27) Å, C(7)–O 1.448(4) vs. 1.397(20) Å, O–Ti 2.295(2) vs. 2.214(10) Å].[2] Meanwhile, the average Ti–Cl distance is nearly the same [2.305(1) Å in **3** vs. 2.308(2) Å in $(\eta^5{:}\eta^1\text{-}O\text{-}C_5H_4CH_2CH_2OCH_3)TiCl_3$]. The sum of the angles

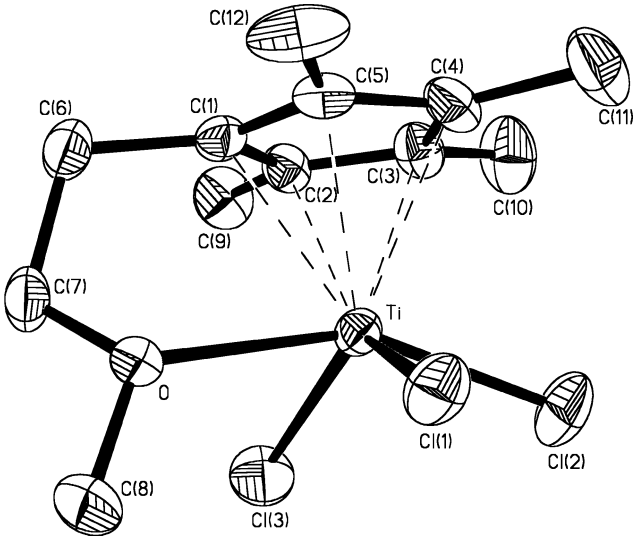

Fig. 1. Molecular structure of complex **3**; displacement ellipsoids are shown at 50% probability level; hydrogen atoms are omitted for clarity; selected bond lengths (Å) and angles (°): Ti–Cl(3) 2.293(2), O–C(8) 1.439(5), Ti–Cl(1) 2.294(1), O–C(7) 1.448(4), Ti–Cl(2) 2.327(1), C(1)–C(6) 1.503(5), Ti–O 2.295(2), C(6)–C(7) 1.510(6); Cl(3)–Ti–Cl(1) 124.44(6), C(8)–O–C(7) 110.7(3), Cl(3)–Ti–Cl(2) 88.04(5), C(8)–O–Ti 120.5(2), Cl(1)–Ti–Cl(2) 88.65(4), C(7)–O–Ti 114.9(2), Cl(2) –Ti– O 153.04(8), C(1)–C(6)–C(7) 110.2(3), Cl(3)–Ti–O 79.56(8), O–C(7)–C(6) 106.1(3), Cl(1)–Ti–O 79.10(7), Ti–Cp_{cent} 2.046.

around the O atom in **3** is 346.1(4)° which is somewhat less than in (η^5:η^1-*O*-$C_5H_4CH_2CH_2OCH_3$)$TiCl_3$ (351.5°).[3] This means that the oxygen atom in **3** is shifted more strongly out of the Ti–C(7)–C(8) plane. Along with the shorter Ti–O distance in (η^5:η^1-*O*-$C_5H_4CH_2CH_2OCH_3$)$TiCl_3$, this is indicative of a weaker effect of the back donation of the second lone-pair of the oxygen atom to the Ti centre in **3** in comparison to its ring non-permethylated analogue (vide infra).

3.1.3. Variable-temperature NMR spectroscopy investigation of the dynamic behaviour of 3 in solutions

Similarly to results reported earlier by Zeijden et al. [12], in a non-solvating medium, complex **3** exhibits a dynamic behaviour due to the reversible intramolecular ether group to metal centre dissociation/coordination (see Scheme 3).

In ^1H and $^{13}C\{^1H\}$ NMR spectra, the lower-field shifts of the signals corresponding to the $-OCH_2-$ and $-OCH_3$ groups are a good criterion for the coordination of the oxygen atom to the titanium centre. Within the whole temperature range studied, no broadening of the

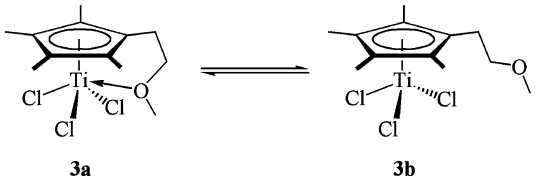

3a **3b**

Scheme 3.

signals is observed, that is indicative of a fast exchange process (NMR time-scale). However, the values of the chemical shifts are strongly temperature dependent (see Fig. 2).

The evaluation of the thermodynamic parameters was performed using Eq. (1),

$$K = \frac{[\text{free}]}{[\text{coord}]} = \exp\left(\frac{\Delta S}{R} - \frac{\Delta H}{RT}\right) = \frac{\delta_{\text{coord}} - \delta(T)}{\delta(T) - \delta_{\text{free}}} \qquad (1)$$

where [coord] and [free] are the molar concentrations of chelate and non-chelate forms of **3** (**3a** and **3b**, respectively), δ_{coord} and δ_{free} are the values of the chemical shifts of 'pure' **3a** and **3b**, and $\delta(T)$ is the observed chemical shift value at temperature T. To perform the evaluation of ΔS and ΔH, the improved r.m.s. non-linear curve fitting procedure for $\delta(T)$ function was applied (see Section 5 for the method modification and computational details). In each series, all four parameters (δ_{coord}, δ_{free}, ΔS and ΔH) were varied. Both of the values (δ and T) were treated as measured with finite accuracies σ_δ and σ_T, respectively, that were assumed to be one and the same within the entire region of interest. The accuracies (r.m.s. deviations) σ_δ and σ_T, were also estimated directly from the empirical data. Remarkably, these estimates are in excellent agreement with the values of the corresponding instrumental errors typical for variable-temperature NMR experiments. The numerical results for the thermodynamic parameters for **3** are given in Table 2.

As one can see from Table 2, the found values for δ_{free} and δ_{coord} are in good agreement with the independent data available from the direct measurements. Thus, for a non-coordinated $-CH_2OCH_3$ moiety, chemical shifts in THF-d_8 can serve as a good comparison point [30 °C, $\delta(^1H) = 3.24$ (OCH_3), 3.51 (OCH_2); $\delta(^{13}C) = 59.09$ (OCH_3), 73.16 (OCH_2)]. As for the chelate form, the chemical shifts of protons and carbon atoms of [η^5:η^1-*O*-$C_5(CH_3)_4CH_2CH_2OCH_3$]$ZrCl_3$ [5] measured in CD_2Cl_2 were considered [30 °C, $\delta(^1H) = 3.70$ (OCH_3), 4.33 (OCH_2); $\delta(^{13}C) = 63.95$ (OCH_3), 82.90 (OCH_2)].

The values of parameters ΔH and ΔS drawn from the $\delta(^{13}C)$ dependencies are in a better mutual agreement than those obtained from the $\delta(^1H)$ ones. In practice, the equilibrium process presented in Scheme 3 is more complicated and one should consider that the solvent molecules also participate in it. Unlike ^{13}C chemical shifts, the proton chemical shifts are markedly influ-

[2] In the crystal, [η^5:η^1-*O*-$C_5H_4CH_2CH_2OCH_3$]$TiCl_3$ possesses two crystallographically independent units in the cell, with C(6) and C(7) carbons disordered in one of them. For comparison, the parameters are taken only for the molecule that possesses no disordered atoms.

[3] Hereinafter, the X-ray structural data not given in original papers were retrieved from CCDC.

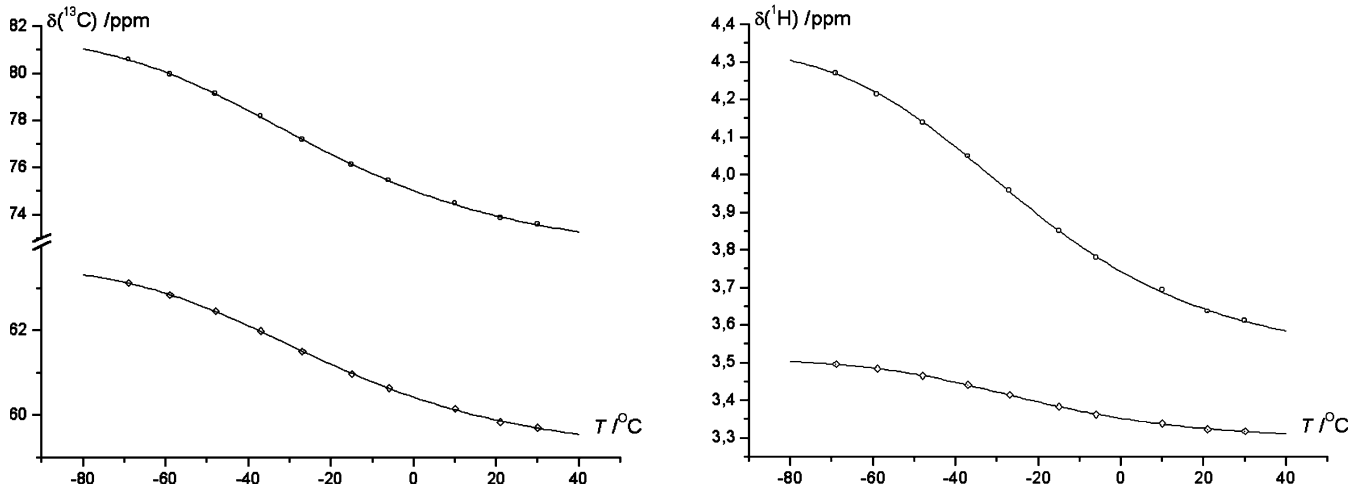

Fig. 2. The optimised $\delta(T)$ dependencies for compound **3**. The plots correspond to the series for nuclei indicated in italic: (**a**) upper curve OCH_3, lower curve CH_2OCH_3; (**b**) upper curve OCH_3, lower curve CH_2OCH_3.

Table 2
The thermodynamic parameters for **3a** and **3b** interconversion process (in CD_2Cl_2). The calculated values δ_{free} and δ_{coord} are also presented

Curve	ΔH (kJ mol^{-1})	ΔS (J mol^{-1} K^{-1})	δ_{free} (ppm)	δ_{coord} (ppm)
$\delta(^1H)$ (OCH_2)	21.8 (0.9)	86.9 (3.8)	3.492 (0.014)	4.341 (0.010)
$\delta(^1H)$ (OCH_3)	25.4 (0.9)	101.0 (3.7)	3.294 (0.003)	3.509 (0.002)
$\delta(^{13}C)$ (OCH_2)	19.7 (1.0)	78.6 (4.2)	72.02 (0.20)	81.58 (0.15)
$\delta(^{13}C)$ (OCH_3)	20.4 (1.0)	80.7 (4.2)	58.95 (0.10)	63.55 (0.07)

enced by the magnetic anisotropy effects induced by the solvent molecules. Thus, from the viewpoint of ^{1}H NMR spectroscopy, the equilibrium in Scheme 3 cannot be treated as a strictly two-site exchange process and Eq. (1) does not work well in this case. Contrarily, the ^{13}C NMR method allows treatment of the equilibrium in question as the true two-site exchange process. Thus, the ΔH and ΔS values obtained from the analysis of the $\delta(^{13}C)$ series seem to be more reliable.

Conclusions that one could draw from comparison of the thermodynamic values for **3** with those reported by Zejden et al. [12] for (η^5:η^1-*O*-$C_5H_4CH_2CH_2O$-CH_3)$TiCl_3$ along with a comparison of the Ti–O bond lengths, at a first glance, are a crude contradiction. For the ring non-permethylated half-sandwich, the enthalpies determined by the numerical analysis of the $\delta(T)$ dependencies are the following: 16.8 (2) kJ mol^{-1} for the (OCH_2) series and 17.6 (5) kJ mol^{-1} for the (OCH_3) one [12]. As one can conclude first, the lower enthalpy values for (η^5:η^1-*O*-$C_5H_4CH_2CH_2OCH_3$)$TiCl_3$ are indicative of the lower Ti–O bond strength compared to that in **3**. However, comparison of the Ti–O bond lengths implies an opposite conclusion.

The point is, however, that the ΔH value corresponds to the entire process and reflects not only the formation of the Ti–O coordination bond, but all changes in the molecular geometry. These changes involving Ti–Cp_{cent} and Ti–Cl (averaged) distances are given in Table 3. As the X-ray structural data for both **3b** and the non-chelated form of (η^5-$C_5H_4CH_2CH_2OCH_3$)$TiCl_3$ are not available, the analogous parameters for the structurally similar (η^5-$C_5H_4CH_3$)$TiCl_3$ and (η^5-$C_5(CH_3)_4CH_2$-CH_3)$TiCl_3$ were retrieved from the Cambridge Structural Database [13] and selected as the reference points.

The data in Table 3 show that the intramolecular coordination of the ether functionality to the metal centre results in the elongation of both the Ti–Cp_{cent} and Ti–Cl distances. However, while the Ti–Cp_{cent} distance elongations are approximately of the same value in both of the cases (+0.024 and +0.026 Å), elongation of the Ti–Cl bonds are noticeably greater for the non-methylated complex (η^5:η^1-*O*-$C_5H_4CH_2$-CH_2OCH_3)$TiCl_3$ than for its ring-permethylated analogue **3a** (+0.085 against +0.062, respectively). Thus, the smaller absolute value ΔH measured for (η^5:η^1-*O*-$C_5H_4CH_2CH_2OCH_3$)$TiCl_3$ comparatively to that for **3a** can be due to the greater weakening of the Ti–Cl bonds in this first complex.

In conclusion, it should be emphasised that the stability of the chelated form **3a** is lower compared to its zirconium analogues (η^5:η^1-*O*-$C_5R_4CH_2$-CH_2OCH_3)$ZrCl_3$ (R = CH_3 [5], H [12]); the latter compounds have their methoxy group always coordinated to the metal atom both in crystalline state and in solutions within the temperature range studied.

Table 3
Comparison of the Ti–Cp_{cent} and Ti–Cl distances for $[\eta^5{:}\eta^1\text{-}O\text{-}C_5R_4\text{-}CH_2CH_2OCH_3]TiCl_3$ (R = H, CH_3) and their non-chelate relatives

Distances	Ring non-permethylated		Ring-permethylated	
	$[\eta^5\text{-}C_5H_4CH_3]\text{-}TiCl_3$	$[\eta^5\text{-}C_5H_4\text{-}CH_2CH_2OCH_3]TiCl_3$	$[\eta^5\text{-}C_5(CH_3)_4\text{-}CH_2CH_3]TiCl_3$	**3a**
Ti–Cp_{cent} (Å)	2.004	2.028 (+0.024) [a]	2.020	2.046 (+0.026)
Ti–Cl [b] (Å)	2.223	2.308 (+0.085)	2.243	2.305 (+0.062)

[a] The bond length elongation caused by the intramolecular coordination are given in brackets.
[b] Averaged distances.

3.2. P-Containing compounds

3.2.1. Synthesis

Similarly to complex **3** the half-sandwich $(\eta^5{:}\eta^1\text{-}P\text{-}C_5H_4CH_2CH_2PPh_2)TiCl_3$ (**6**) was prepared via the trimethylsilyl substituted cyclopentadiene **5**, as it is depicted in Scheme 4.

Silane **5** smoothly reacts with $TiCl_4$ in toluene at room temperature to give a poorly-soluble product separating from the reaction mixture as a finely-crystalline voluminous orange 'wool' sensitive to air and moisture. It is remarkable that the composition of **6** as an adduct with toluene $(\eta^5{:}\eta^1\text{-}P\text{-}C_5H_4CH_2CH_2PPh_2)TiCl_3\cdot C_6H_5CH_3$ (analysis of the ^1H and $^{13}C\{^1H\}$ NMR spectral data) surprisingly does not change after crystallisation from a minimum amount of hot THF. However, if crystallised from CH_2Cl_2, no toluene is included into the crystal lattice and its signals are not observed in the NMR spectra.

3.2.2. X-ray structural investigation of 6

Single crystals of **6** were obtained by crystallisation from dichloromethane as an adduct with 1/2 molecule of CH_2Cl_2 lying on crystallographic two-fold axes. In the crystalline state, complex **6** exhibits the same coordination polyhedron of the metal centre as that was observed for **3**, i.e. the 'four-leg piano stool' in which the phosphorous atom occupies one of the positions at the base of the pyramid. The molecular structure of **6** is given in Fig. 3. Of interest, its formerly reported zirconium analogue $(\eta^5{:}\eta^1\text{-}P\text{-}C_5H_4CH_2CH_2PPh_2)\text{-}ZrCl_3\cdot THF$ possesses the six-coordinated metal centre, with the THF molecule occupying one of the apical positions of the distorted tetragonal bipyramid [4].

The Ti–P bond length (2.627(2) Å) is slightly longer than in $(\eta^5\text{-}C_5H_5)TiCl_3[P(CH_3)_3]$ (2.604(3) Å) [14] and nearly the same as in $(\eta^5\text{-}C_5H_5)TiCl_2[\eta^1{:}\eta^1\text{-}O,P\text{-}OC_6H_3(2\text{-}Bu^t)(6\text{-}PPh_2)]$ (2.624(3) Å) [15], with both complexes exhibiting the same spatial configuration as **6**. Comparison of the bond angles in the coordination environment of the phosphorous atom in **6** and its zirconium analogue $(\eta^5{:}\eta^1\text{-}P\text{-}C_5H_4CH_2CH_2PPh_2)\text{-}ZrCl_3\cdot THF$ indicates that the pseudo five-membered metallocycle in **6** is less constricted spatially. Indeed, the range of the angles at the P-atom in the titanium complex **6** is 19° (100.2°–119.2°) while in the zirconium complex this range is 23° (101.9°–124.7°) [4].

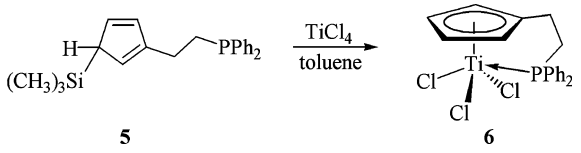

5 6

Scheme 4.

3.2.3. Variable-temperature NMR spectroscopy investigation of the dynamic behaviour of 6 in solutions. Comparison with that for its Zr-analogue

Complex **6** was studied by $^{31}P\{^1H\}$ NMR spectroscopy in both solvating (THF-d_8) and non-solvating (CD_2Cl_2) media within a broad range of temperatures.[4] The lower field shifting of $\delta(^{31}P)$ values is a good

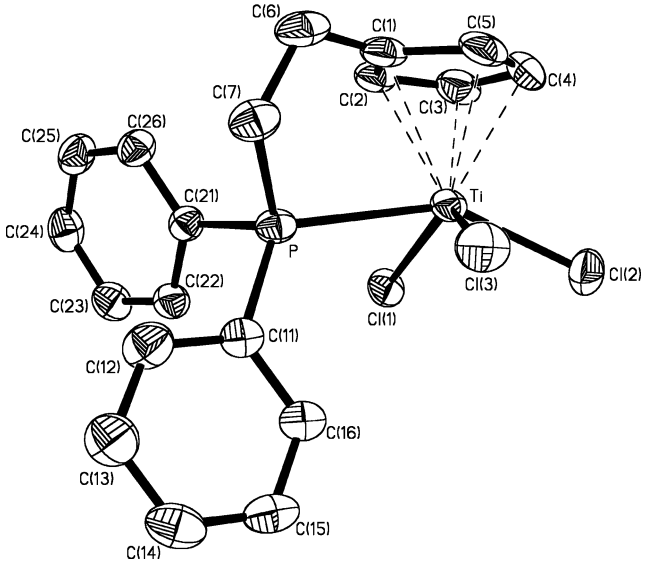

Fig. 3. Molecular structure of complex **6**; displacement ellipsoids are shown at 50% probability level, hydrogen atoms and solvent dichloromethane molecule are omitted for clarity; selected bond lengths (Å) and angles (°): Ti–Cl(1) 2.310(2), P–C(7) 1.837(4), Ti–Cl(2) 2.326(1), P–C(11) 1.817(3), Ti–Cl(3) 2.329(2), P–C(21) 1.819(3), Ti–P 2.627(2); Cl(1)–Ti–Cl(2) 87.19(5), C(11)–P–C(21) 100.2(2), Cl(1)–Ti–Cl(3) 129.63(6), C(11)–P–C(7) 106.7(2), Cl(2)–Ti–Cl(3) 88.31(5), C(21)–P–C(7) 107.5(2), Cl(1)–Ti–P 80.30(6), C(11)–P–Ti 118.6(1), Cl(2)–Ti–P 148.07(4), C(21)–P–Ti 119.2(1), Cl(3)–Ti–P 77.70(5), C(7)–P–Ti 103.8(2), C(1)–C(6)–C(7) 114.9(3), C(6)–C(7)–P 110.8(3), Ti–Cp_{cent} 2.035.

criterion for the coordination of the phosphanyl group towards the metal centre, while the chemical shift of a free $-CH_2PPh_2$ group [$\delta(^{31}P) \cong -14$] [4] was chosen as a comparison point.

In non-solvating CD_2Cl_2, no evidence of any dynamic behaviour was found. The chemical shift of the PPh_2 group changes slightly (from $\delta(^{31}P) = 27.1$ at $+30\ ^\circ C$ to $\delta(^{31}P) = 32.1$ at $-78\ ^\circ C$), with no considerable broadening of signal observed. This is indicative of the retention of Ti←P coordination in a non-solvating medium within the entire temperature range studied. In an *n*-donor solvent, however, the situation changes dramatically. The observed variation of $\delta(^{31}P)$ exceeds 30 ppm (from $\delta(^{31}P) = -2.1$ at $+60\ ^\circ C$ to $\delta(^{31}P) = +29.7$ at $-78\ ^\circ C$, see Fig. 4).

It is apparent, that in contrast to what was observed for **3,** the n-donor solvent molecule assists the equilibrium process of the pendant phosphanyl group intramolecular dissociation-coordination (see Scheme 5).

Accordingly to this Scheme 5, Eq. (1) should be changed to

$$K = \frac{n_{free}}{n_{THF} n_{coord}} \frac{[free]([THF] + [coord] + [free])}{[coord][THF]} = \exp\left(\frac{\Delta S}{R} - \frac{\Delta H}{RT}\right) = \frac{\delta_{coord} - \delta(T)}{\delta(T) - \delta_{free}} \quad (2)$$

where n_{coord}, n_{free} and n_{THF} are the molar fractions of the corresponding components in the equilibrium mixture, square bracketed values are the corresponding molar equilibrium concentrations of the chelated and non-chelated forms of **6** (**6a** and **6b**, respectively) and the

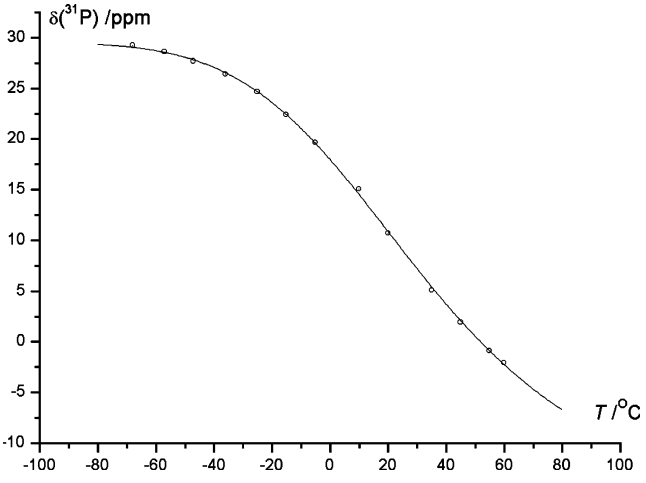

Fig. 4. The optimised $\delta(T)$ dependencies for compound **6** in THF.

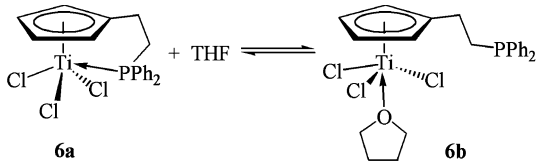

Scheme 5.

solvent concentration.[5] Actually, the estimated value of [THF]/([THF]+[coord]+[free]) for the experimental conditions is only 0.99 which causes only approximately 0.1 J mol^{-1} K^{-1} correction for the ΔS parameter. Taking into account the final r.m.s. deviations for ΔS, this correction can be easily neglected. Thus, in this case, the computation of the parameters ΔS, ΔH, δ_{free} and δ_{coord} was performed similarly to that for **3**. The found values are the following: $\Delta H = 23.4$ (2.3) kJ mol^{-1} K^{-1}, $\Delta S = 76.5$ (7.3) J mol^{-1} K^{-1}, $\delta_{free} = -17.41$ (5.99), $\delta_{coord} = 29.55$ (0.22). The more accurate and trustworthy value for δ_{coord} than for δ_{free} (compare with $\delta(^{31}P)$ of complex **6** in CD_2Cl_2 and $\delta(^{31}P)$ of the free PPh_2 group, vide supra), evidently, is due to the fact that the empirical points could be in practice measured only for the lower-temperature branch of the computed curve, with the higher-temperature part of the curve remaining unavailable because of the boiling point of the solvent used.

The obtained data are worthwhile to be discussed from two viewpoints. Their comparison for complexes **6** and (η^5:η^1-*O*-$C_5H_4CH_2CH_2OCH_3$)$TiCl_3$ [11,12] reveals that the ether group exerts a lower affinity towards the Ti(IV) centre than the phosphanyl group. The dissociation of the ether group takes place in the non-solvating medium (CD_2Cl_2), while the PPh_2 group in the same solvent remains coordinated to the Ti(IV) centre and exhibits hemilability only in THF. In a THF solution of **3**, the coordination of an intramolecular ether moiety to the Ti(IV) centre is not observed at all. Most likely, the same would be observed for (η^5:η^1-*O*-$C_5H_4CH_2CH_2OCH_3$)$TiCl_3$, if its spectra in THF-d_8 were measured.

The great positive value of ΔS observed for **6** [76.5 (7.3) J mol^{-1} K^{-1}] (compare to 79 J mol^{-1} K^{-1} for **3** and 66 J mol^{-1} K^{-1} for (η^5:η^1-*O*-$C_5H_4CH_2CH_2OCH_3$)$TiCl_3$ [12]) is also noteworthy. One should keep in mind, that in the case of **6**, the solvent molecule is captured by the metal centre along with the dissociation of the PPh_2 group. This fact could be accounted for by a considerable loss in entropy due to the loss of the rotational freedom degrees of the phenyl rings in the PPh_2–group when coordinated.

[4] Series of the variable-temperature ^1H and $^{13}C\{^1H\}$ NMR spectra were also measured. However, the appearance of the signals in the $-CH_2CH_2PPh_2$ region is complicated due to the strong coupling with the phosphorous nucleus. This made it impossible to measure $\delta(^1H)$ and $\delta(^{13}C)$ with the required accuracy.

[5] Application of the molar fractions makes the value *K* non-dimensional.

Comparison of **6** with its Zr analogue (η^5:η^1-*P*-$C_5H_4CH_2CH_2PPh_2$)$ZrCl_3$ [4] indicates their markedly different dynamic behaviour in the solvating media. Thus, while in the Zr complex the coordinated PPh_2 group is replaced by the second THF molecule with a decrease of temperature (see Scheme 6), the same decrease of temperature in the case of **6** leads to a different result (see Scheme 5). Thus, the enthalpy changes for the intramolecular coordination-dissociation of the PPh_2 group in **6** and in (η^5:η^1-*P*-$C_5H_4CH_2CH_2PPh_2$)$ZrCl_3$ have opposite signs. This allows one to conclude that the intramolecular Ti←P bond in **6** is more stable than the analogous Zr←P bond in (η^5:η^1-*P*-$C_5H_4CH_2CH_2PPh_2$)$ZrCl_3$. Apparently, one should consider that this comparison is to be done with care because of the different coordination polyhedrons in all of the forms of **6** and in those of (η^5-$C_5H_4CH_2CH_2PPh_2$)$ZrCl_3$. Nevertheless, the opposite trends of the coordination abilities for ether and phosphanyl groups towards Ti(IV) and Zr(IV) centres are rather clear. Thus, while the Zr(IV) metal centre exhibits a greater affinity towards the ether-type oxygen atom than to P-atom in the phosphanyl group, for the Ti(IV) metal centre this tendency is opposite.

Here it is illustrative to present our previously unpublished data on the dynamic behaviour of (η^5:η^1-*P*-$C_5(CH_3)_4CH_2CH_2PPh_2$)$ZrCl_3$·THF reported earlier [8]. Unlike (η^5:η^1-*P*-$C_5H_4CH_2CH_2PPh_2$)$ZrCl_3$, ring-permethylated Zr(IV) half-sandwich complex (η^5:η^1-*P*-$C_5(CH_3)_4CH_2CH_2PPh_2$)$ZrCl_3$·THF exhibits no dynamic behaviour in all suitable solvents tested. The $\delta(^{31}P)$ value remains nearly unchanged with a decrease of temperature from 30 °C (2.9) to −87 °C (3.9) (the data for THF-d_8; in CD_2Cl_2 $\delta(^{31}P) = 5.8$ at 30 °C). Thus, in (η^5:η^1-*P*-$C_5(CH_3)_4CH_2CH_2PPh_2$)$ZrCl_3$·THF no substitution of the PPh_2 group with a second THF molecule is observed as takes place in (η^5:η^1-*P*-$C_5H_4CH_2CH_2PPh_2$)$ZrCl_3$·THF. Meanwhile, the Zr–P distance in (η^5:η^1-*P*-$C_5(CH_3)_4CH_2CH_2PPh_2$)$ZrCl_3$·THF (2.8906(11) Å) [8] is greater than that in (η^5:η^1-*P*-$C_5H_4CH_2CH_2PPh_2$)$ZrCl_3$·THF (2.8474(5) Å) [4]. The distance from the Zr atom to the mean plane of the Cp ring and the Zr–O(THF) bond length in [η^5:η^1-*P*-$C_5(CH_3)_4CH_2CH_2PPh_2$]$ZrCl_3$·THF [2.256(1) and 2.419(2) Å, respectively] are also longer than those in (η^5:η^1-*P*-$C_5H_4CH_2CH_2PPh_2$)$ZrCl_3$·THF (2.236(1) and 2.3613(12) Å, respectively). However, the average Zr–Cl distance in (η^5:η^1-*P*-$C_5(CH_3)_4CH_2CH_2PPh_2$)$ZrCl_3$·THF (2.473(5) Å) is shorter than that in the ring non-permethylated analogue (2.4866(3) Å).[6] This resembles strongly what is observed for Ti complexes **3** and (η^5:η^1-*P*-$C_5H_4CH_2CH_2OCH_3$)$TiCl_3$. It is illustrative for the fact that the thermodynamic stability of the chelate form of a complex may not correlate (as it is considered usually) with the length of the metal–heteroelement coordination bond. However, this last parameter may be considered a good one for the determination of the relative metal–heteroatom bond strengths within a row of similarly constructed compounds.

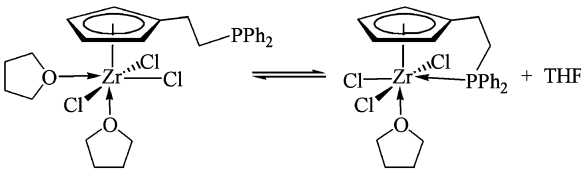

Scheme 6.

4. Conclusion

The performed investigation allows to confirm, that in solution, the chelate form of complexes (η^5-*O*-$C_5R_4CH_2CH_2OCH_3$)MCl_3 (R = H, CH_3; M = Ti, Zr) is more stable for the Zr complexes. Comparison of O- and P-side-chain functionalized Ti(IV) and Zr(IV) half-sandwich complexes reveals the opposite tendencies in the stability of the chelate forms in solutions. While the Zr(IV) metal centre exhibits a greater affinity to the ether type oxygen atom, for the Ti(IV) metal centre the intramolecular coordination with the phosphanyl group appears to be more preferable. Finally, comparison of the X-ray structural analysis data along with the thermodynamic parameters of the intramolecular coordination-dissociation equilibrium processes in solution for both (η^5:η^1-*O*-$C_5R_4CH_2CH_2OCH_3$)$TiCl_3$ (R = H, CH_3) and (η^5:η^1-*P*-$C_5R_4CH_2CH_2PPh_2$)$ZrCl_3$·THF (R = H, CH_3) revealed that the thermodynamic stability of the chelate forms of these compounds do not correlate directly with the metal–heteroatom coordination bond length. From our viewpoint, this is due to the fact that the thermodynamics of the processes is contributed not only by the formation-cleavage of the metal–heteroatom coordination bond, but to a larger extent, by the electron and structural reorganisation of the complex in general.

5. Supplementary material

Supplementary material for this article include the details of the numerical processing of the variable-temperature NMR data and is available from authors on request.

Crystallographic data for the structural analysis have been deposited with the Cambridge Crystallographic

[6] For (η^5-$C_5H_4CH_2CH_2PPh_2$)$ZrCl_3$·THF the data are given only for one of the crystalline modifications. In the second modification that possesses two crystallographically independent molecules, the analogous parameters are nearly of the same value.

Data Centre, CCDC Nos. 194203 and 194204. Copies of this information may be obtained free of charge from The Director, CCDC, 12 Union Road, Cambridge, CB2 1EZ, UK (fax: +44-1223-336033; e-mail: deposit@ccdc.cam.ac.uk or www: http://www.ccdc.cam.ac.uk).

Acknowledgements

The authors of the paper are deeply thankful to Prof. Georgievskii D.V. (Dept. of Mechanics and Mathematics, M.V. Lomonosov Moscow State University) for his kind advices and help in preparing of the computational part (Section 5) of the paper. The authors greatly acknowledge the Russian Foundation for Basic Research for CSD licence payment (grant 02-07-90322) and financial support for A.V.C. (grant 01-03-32474).

References

[1] U. Siemeling, Chem. Rev. 100 (2000) 1495.
[2] H. Butenschön, Chem. Rev. 100 (2000) 1527.
[3] C. Müller, D. Vos, P. Jutzi, J. Organometal. Chem. 600 (2000) 127.
[4] D.P. Krut'ko, M.V. Borzov, E.N. Veksler, A.V. Churakov, J.A.K. Howard, Polyhedron 17 (1998) 3889.
[5] D.P. Krut'ko, M.V. Borzov, V.S. Petrosyan, L.G. Kuz'mina, A.V. Churakov, Russ. Chem. Bull. 45 (1996) 1740.
[6] D.P. Krut'ko, M.V. Borzov, V.S. Petrosyan, L.G. Kuz'mina, A.V. Churakov, Russ. Chem. Bull. 45 (1996) 940.
[7] D.P. Krut'ko, M.V. Borzov, E.N. Veksler, R.S. Kirsanov, A.V. Churakov, D.A. Lemenovskii, Pure and Appl. Chem. 73 (2001) 367.
[8] D.P. Krut'ko, M.V. Borzov, E.N. Veksler, R.S. Kirsanov, A.V. Churakov, Eur. J. Inorg. Chem. (1999) 1973.
[9] P. Jutzi, J. Dahlhaus, Synthesis (1993) 684.
[10] E.E.C.G. Gielens, J.Y. Tiesnitsch, B. Hessen, J.H. Teuben, Organometallics 17 (1998) 1652.
[11] Q. Huang, Y. Qian, G. Li, Y. Tang, Transition Met. Chem. 15 (1990) 483.
[12] A.A.H. van der Zeijden, C. Mattheis, R. Fröhlich, Organometallics 16 (1997) 2651.
[13] F.H. Allen, O. Kennard, Chem. Autom. Des. News 8 (1993) 31.
[14] T.T. Nadasdi, D.W. Stephan, Inorg. Chem. 32 (1993) 5933.
[15] C.A. Willoughby, R.R. Daff, Jr, W.M. Davis, S.L. Buchwald, Organometallics 15 (1996) 472.
[16] G.M. Sheldrick, Acta Crystallogr., Sect. A 46 (1990) 467.
[17] G.M. Sheldrick, SHELXL-93: Program for the Refinement of Crystal Structures, University of Göttingen, Germany, 1993.